JOURNAL OF CATALYSIS 86, 239–244 (1984)

Evidence for Alkyl Intermediates during Fischer–Tropsch Synthesis and Their Relation to Hydrocarbon Products

CHIAZUAN JEFF WANG AND JOHN G. EKERDT[1]

Department of Chemical Engineering, The University of Texas at Austin, Austin, Texas 78712

Received April 15, 1983; revised November 7, 1983

Fischer–Tropsch synthesis mechanisms have been postulated in which alkyl fragments are both the chain-growing intermediate and the precursor to hydrocarbon products. The conversion of CO/H_2 into small alkyl fragments was investigated by scavenging C_1–C_3 alkyl species from the surface of an iron catalyst during Fischer–Tropsch synthesis. The experiments were performed in a steady-state mode revealing that pyridine did not inhibit or poison the Fischer–Tropsch reaction, rather it suppressed the overall rate slightly. Scavenged α-alkylpyridine distributions were dependent upon synthesis variables and displayed a dependence which was proportional to the dependence of C_1–C_3 Fischer–Tropsch products. These dependences are used to demonstrate that alkyl fragments are the immediate precursors to Fischer–Tropsch products.

I. INTRODUCTION

In a recent study of Fischer–Tropsch synthesis we reported the catalytic behavior of Fe/SiO_2 and the development of a reactive scavenging technique with pyridine (*1*). Experiments demonstrated that pyridine interacted with methyl and ethyl species to produce α-methyl- and α-ethylpyridine. These alkyl species were formed from CO and H_2 on the iron surface and were scavenged from the iron surface.

The scavenging technique can provide unique insight into the Fischer–Tropsch reaction mechanism. The technique has been used to identify reaction intermediates (*2, 3*). Furthermore, the distribution of substituted scavenger molecules should be a reflection of the distribution of intermediates. Langmuir–Hinshelwood mechanisms have been constructed to describe propagation, and olefin and alkane formation from a common alkyl species (*4*). These mechanisms can be used to predict distributions of surface intermediates. Alkyl-substituted scavenger distributions represent a second set of data against which to test the reasonableness of postulated mechanisms. A mechanism must describe Fischer–Tropsch product and intermediate species distributions.

The means by which CO and H_2 interact over a catalyst to give C_2 and higher products is the subject of active investigation. The two most likely mechanisms, which have been discussed in recent reviews (*5, 6*), are presented in Fig. 1. Both involve chain-growth steps in which an alkyl fragment undergoes either addition or termination. Definitive experiments have not been performed which prove either mechanism (*7*). While the evidence is indirect (*8, 9*), the scheme involving methylene insertion appears to be the correct mechanism under most conditions.

It has not been possible to discriminate between the mechanisms by analyzing the dependence of steady-state product distributions upon the postulated reaction variables, reactant partial pressures and temperature. The mechanisms contain a common intermediate, alkyl species, which have been scavenged from iron (*1*) and ruthenium catalysts (*2, 3*). The studies reported herein were directed toward determining the effect of the synthesis variables

---

[1] To whom correspondence should be addressed.

0021-9517/84 $3.00

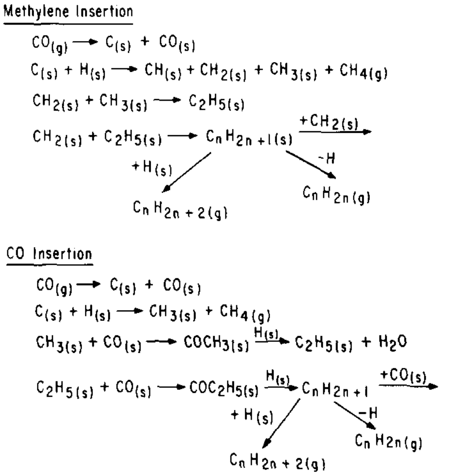

FIG. 1. Possible Fischer–Tropsch reaction mechanisms.

on the distribution of alkyl fragments over an iron catalyst and using these measured effects to gain insight into the role alkyl fragments have in the Fischer–Tropsch synthesis reaction.

II. METHODS

The experimental apparatus, microreactor, catalyst preparation and conditioning, and hydrocarbon analysis procedures are described elsewhere (*1*). The experiments were performed at 230°C, 1.54 atm of total pressure (1 atm equals 101.3 kPa), and 14,700 WHSV (gas flow rate at the inlet conditions in $cm^3/h/g$ of catalyst). Carbon monoxide conversion never exceeded 2%.

The catalyst, 20.44 wt% Fe_2O_3/SiO_2, was conditioned for 6 days at 230°C under a 4/1 H_2/CO mixture prior to any scavenging. This produced a catalyst which displayed a stable steady-state activity. X-Ray diffraction (XRD) analysis indicated the presence of Fe_3O_4 and ε'-carbide, $Fe_{2.2}C$, after the conditioning (*1*). The surface area of the working catalyst was not determined. The Fe_2O_3 had a crystallite size of 240 Å which resulted in approximately 80–100 μmol of surface sites of Fe_2O_3 being charged to the reactor. The catalyst was allowed to adjust to new-synthesis conditions for 6 h before data were collected.

The scavenging protocol was altered from our earlier paper (*1*). Pyridine was injected continuously because this resulted in a constant-surface scavenger concentration and scavenged distributions represented a steady-state condition. For continuous injection, He at 2 sccm was sparged through a stainless-steel frit at 0°C and combined with the feed to the reactor. The effect of helium flow and saturator temperature were not studied, the conditions were selected to enhance saturation and minimize pyridine partial pressure. The saturator was fabricated from copper because the saturation was conducted at 1.68 atm. Pyridine formed a complex with copper which darkened the solution. Identical results were obtained with fresh pyridine, copper-contaminated pyridine, or pyridine in a glass sparger. The reactor effluent was trapped at liquid-nitrogen temperature for 25 min.

Trapped products were washed from the inside of the 50-ml collection flask with 0.05 ml of diethyl ether. One to five microliters of the ether solution was injected into a capillary column. The products were separated using an amine-deactivated fused silica column (0.25 mm I.D. × 30 m) loaded with Carbowax. A nitrogen–phosphorus detector (NPD) was used to detect nitrogen-containing compounds. Details of product identification are given elsewhere (*1, 10*). Three samples were injected for each experiment; average values are reported. Amounts of a given nitrogen-containing compound were related directly to the NPD signal area.

III. RESULTS AND DISCUSSION

The major components detected in the scavenged samples were pyridine, 2-methylpyridine, 2,6-dimethylpyridine, 2-ethylpyridine, and 2-propylpyridine. The 2,6-dimethylpyridine signal was less than 2.5% of the 2-methylpyridine signal. 2-Butylpyridine was detected occasionally, however, the signal-to-noise ratio for this peak was

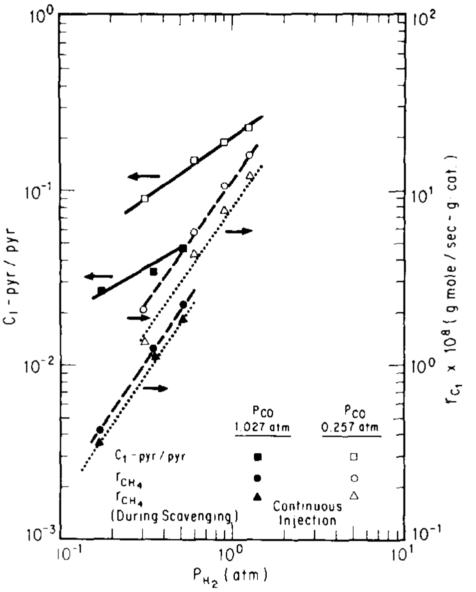

FIG. 2. C_1-Pyridine/pyridine and the rate of methane formation dependence on the partial pressure of H_2, where (———) represents the methane formed in the absence of pyridine and (· · ·) represents methane formed during continuous pyridine injection.

insufficient for quantitative purposes. Trace amounts of 4-ethylpyridine and what was thought to be a methylethylpyridine were observed. The last two component signals were too weak to quantify. Pyridine was not found to undergo hydrogenation at the conditions of this study (*1*).

Studies of the adsorbed states of pyridine on iron films have demonstrated that pyridine bonds to a preoxidized iron surface through the nitrogen lone-pair electrons and to a clean iron surface through π electrons (*11*). Conditioned catalysts were analyzed by XRD and found to consist of bulk iron carbides and possibly some Fe_3O_4. The surface was not analyzed; the presence of some Fe_3O_4 at the surface was postulated on the basis of water-gas shift activity (*1*). The means by which pyridine adsorbed on the surface may be inferred from the fact that almost all products were substituted at the 2 position. This suggests that pyridine adsorbed through nitrogen.

The details and efficiency of the reaction between adsorbed pyridine and alkyl are unknown. The reaction to 2-C_n-pyridine is thought to occur between an n-alkyl fragment containing n carbon atoms and pyridine (*12, 13*). The scavenged distributions C_n-pyridine/C_{n+1}-pyridine decreased rapidly with increasing n and butylpyridine was difficult to detect. This decrease may have been caused by the actual distribution of alkyl fragments and/or by steric limitations between larger alkyl fragments and pyridine. Steric limitations are suspected; however, because known alkyl distributions could not be generated the steric effects could not be quantified. Scavenging experiments were performed at one temperature to avoid assigning alkyl distribution changes with temperature to possible changes in the relative rates of the scavenging reactions.

The absolute amount of pyridine injected was held constant. The amount collected and ultimately injected into the capillary column varied because these operations required several manual manipulations. A suitable internal standard could not be identified therefore, for consistency all alkylpyridine signals were normalized with the signal of pyridine. These normalized signals are used to examine effects of the synthesis variables on the alkyl fragments. The trends reflect changes in surface alkyl concentrations; the absolute magnitude of a scavenged distribution at one set of conditions does not reflect the absolute magnitude of the surface alkyl distribution.

The effects of reactant partial pressure on the sum of 2-methylpyridine and two times 2,6-dimethylpyridine to pyridine (C_1-pyridine/pyridine) and methanation activity are shown in Figs. 2 and 3. The partial pressures were selected to produce nominal H_2/CO ratios of 5/1 to 1/1 for P_{CO} equal to 0.257 atm or P_{H_2} equal to 0.77 atm and nominal ratios of 1/1 to 0.2/1 for P_{CO} equal to 1.027 atm or P_{H_2} equal to 0.308 atm. These figures demonstrate that the rate of methane formation was suppressed slightly in the presence of pyridine. Similar phenomena were

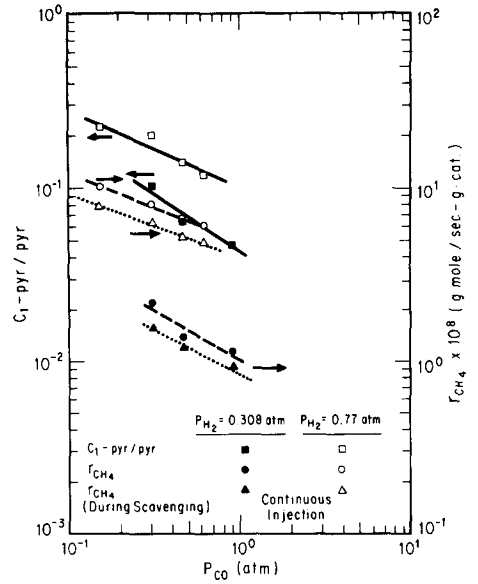

FIG. 3. C_1-Pyridine/pyridine and the rate of methane formation dependence on the partial pressure of CO, where (---) represents the methane formed in the absence of pyridine and (· · ·) represents methane formed during continuous pyridine injection.

observed for the rates of C_2, ethane and ethylene, and C_3, propane and propylene, formation. The rate suppressions were expected since pyridine was titrating small alkyl fragments from the surface. (Fischer–Tropsch activity was always recovered in the absence of pyridine.)

Pyridine did not noticeably alter the C_1–C_6 distribution for both pulse (*1*) and continuous injection but did affect the olefin/alkane ratio. In all cases the low-weight Fischer–Tropsch products were more olefinic during pyridine injection. The olefin/alkane ratio was found to increase with increasing P_{CO} and decreasing P_{H_2}. The olefin/alkane partial pressure dependences (*10*) were nearly the same in the presence and absence of pyridine. Wedler *et al.* (*14*) found that CO displaced preadsorbed H_2 from polycrystalline iron films. The increasing olefin content with CO and pyridine over our catalyst may have been caused by the displacement of surface hydrogen by either species. Displacement of surface hydrogen would also account for some of activity suppression when pyridine was present.

The partial pressure dependences of the rates of CH_4 (Figs. 2 and 3) and C_2 and C_3 hydrocarbons appeared the same in the presence and absence of pyridine. The similar partial pressure dependences for the rates and olefin/alkane ratios demonstrate that Fischer–Tropsch synthesis continued in the presence of pyridine. The absence of a noticeable effect of pyridine on reactant power-law dependences also suggests that the Fischer–Tropsch mechanism was not affected by the presence of pyridine.

Figure 2 shows that the rate of methane formation had a greater H_2 partial pressure dependence that did C_1-pyridine. The methane rate depended on P_{H_2} to the 1.5 power, whereas C_1-pyridine had powers of 0.9 and 0.6 for P_{CO} equal to 0.257 and 1.027 atm, respectively. The P_{CO} dependences for CH_4 and C_1-pyridine were nearly identical (Fig. 3).

These results are qualitatively consistent with methane formation occurring via methyl hydrogenation, viz.,

$$CH_{3(s)} + H_{(s)} \rightarrow CH_{4(g)} \qquad (1)$$

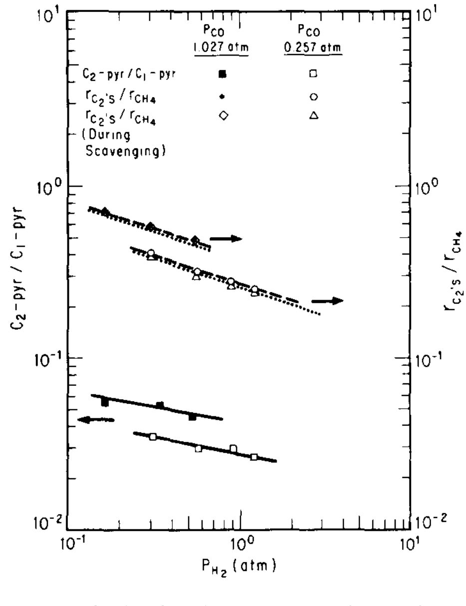

FIG. 4. Distribution dependence of C_2 and C_1 scavenged and Fischer–Tropsch products on the partial pressure of H_2.

Assuming that molecular CO occupies some surface sites, that CO is more strongly adsorbed than H and that H_2 adsorbs dissociatively results in the coverage of H depending on P_{H_2} to the 0.5 power (*10*). When methane has a 1.5 P_{H_2} dependence the surface CH_3 concentration (C_1-pyridine) should depend on P_{H_2} to the 1.0 power.

The effects of reactant partial pressures on the rates of C_2 and C_3 Fischer–Tropsch product formation and on 2-ethylpyridine (C_2-pyridine) and 2-propylpyridine (C_3-pyridine) were also determined. The partial-pressure dependence on H_2 was positive for all rates and scavenged products; the dependence was less for the C_n-pyridine than for the corresponding rate of total C_n production. All species displayed a negative P_{CO} dependence; the C_n-pyridine dependence was more negative.

Figures 4–7 present the distribution dependences of the alkylpyridines and the Fischer–Tropsch products on reactant partial pressures. Except for the data collected at P_{CO} of 0.257 atm on Fig. 5 the distribution of scavenged products and the ratios of the hydrocarbon rates displayed nearly the same pressure dependences. Previous work (*1*) had established that pyridine was reacting with reaction intermediates rather than with Fischer–Tropsch products.

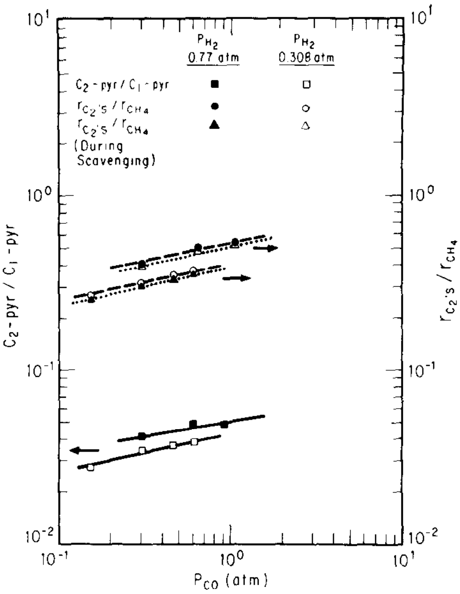

FIG. 6. Distribution dependence of C_2 and C_1 scavenged and Fischer–Tropsch products on the partial pressure of CO.

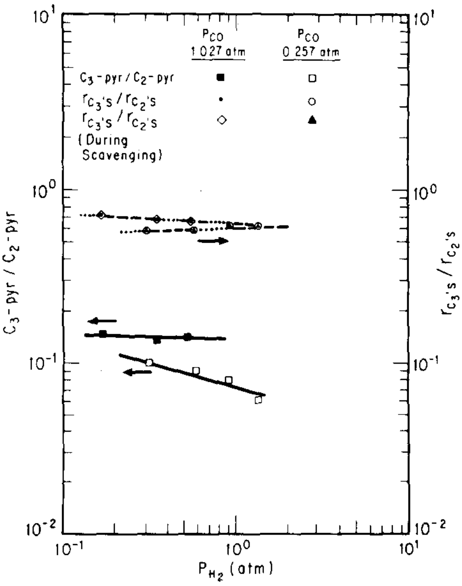

FIG. 5. Distribution dependence of C_3 and C_2 scavenged and Fischer–Tropsch products on the partial pressure of H_2.

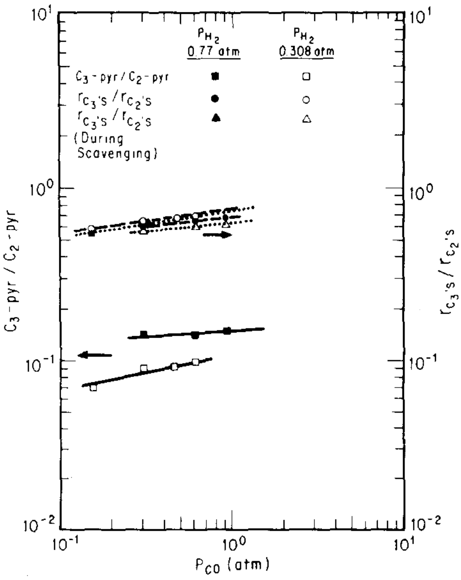

FIG. 7. Distribution dependence of C_3 and C_2 scavenged and Fischer–Tropsch products on the partial pressure of CO.

Kellner and Bell (*4*) presented detailed kinetic arguments using the methylene insertion mechanism in which they showed that the ratio θ_{n+1}/θ_n equaled the chain-growth parameter α, where θ_n represents the surface coverage of an alkyl fragment of carbon number n. They also showed that when the termination rate constants are independent of the carbon number n the ratio of θ_{n+1}/θ_n equals the ratio of total C_{n+1}/C_n hydrocarbon production for $n \geq 2$. The chain-growth parameter and C_{n+1}-pyridine/C_n-pyridine should have the same partial-pressure dependences. Correspondence between C_{n+1}-pyridine/C_n-pyridine and the rate ratio C_{n+1}/C_n implies that the termination rate constants for $n + 1$ and n were similar.

Langmuir–Hinshelwood expressions for alkyl fragment concentrations and for the chain-growth parameter were developed for the two postulated mechanisms shown in Fig. 1 (*10*). The resulting expressions for α were compared with the experimental ratios of C_{n+1}-pyridine/C_n-pyridine (Figs. 4–7) to determine which growth mechanism predominated. It was not possible to discriminate between the mechanisms because the P_{CO} dependence of the CO coverage at reaction conditions could not be determined. Both mechanisms were in qualitative agreement with the data, therefore, the studies support a mechanism in which alkyl fragments are involved in the propagation step.

Pyridine scavenged alkyl fragments. The ratio of C_{n+1}-pyridine/C_n-pyridine was proportional to the ratio of θ_{n+1}/θ_n. As discussed earlier, trends in the alkylpyridine ratios were expected to represent trends in the surface alkyl concentrations. The correspondence between the alkylpyridine ratios and the Fischer–Tropsch product ratios demonstrates that alkyl fragments are the immediate Fischer–Tropsch product precursors.

IV. CONCLUSION

Pyridine has been shown to be an effective scavenger which reacted with Fischer–Tropsch synthesis intermediates, alkyl species. Pyridine did not significantly affect Fischer–Tropsch activity therefore the scavenged alkyl species were representative of species present during synthesis in the absence of pyridine. The resulting alkylpyridine distributions were used to determine the dependence of the reactant partial pressures on the alkyl species. This research has demonstrated that alkyl species are reaction intermediates for the Fischer–Tropsch synthesis reaction and are the immediate precursors to alkanes and olefins.

ACKNOWLEDGMENTS

This work was supported by the Division of Chemical Sciences, Office of Basic Energy Sciences, U.S. Department of Energy under Contract DE-AS05-80ER1072. The University of Texas Center for Energy Studies provided support for the gas chromatograph.

REFERENCES

1. Wang C. J., and Ekerdt, J. G., *J. Catal.* **80,** 172 (1983).
2. Ekerdt, J. G., and Bell, A. T., *J. Catal.* **62,** 19 (1980).
3. Baker, J. A., and Bell, A. T., *J. Catal.* **78,** 165 (1982).
4. Kellner, C. S., and Bell, A. T., *J. Catal.* **70,** 418 (1981).
5. Biloen, P., and Sachtler, W. M. H., "Advances in Catalysis," Vol. 30, p. 163. Academic Press, New York, 1981.
6. Bell, A. T., *Catal. Rev. Sci. Eng.* **23,** 203 (1981).
7. Henrici-Olive, G., and Olive, S., *J. Mol. Catal.* **16,** 111 (1982).
8. Brady, R. C., and Pettit, R., *J. Amer. Chem. Soc.* **102,** 6181 (1980).
9. Brady, R. C., and Pettit, R., *J. Amer. Chem. Soc.* **103,** 1287 (1981).
10. Wang, C. J., "Study of Fischer–Tropsch Synthesis Over a Silica Supported Iron Catalyst Through the Use of Reactive Scavengers," Ph.D. thesis, Department of Chemical Engineering, University of Texas, Austin, Texas, 1983.
11. Kishi, K., Chinomi, K., Inoue, Y., and Ikeda, S., *J. Catal.* **60,** 228 (1979).
12. Reinecke, M. G., and Kray, L. R., *J. Amer. Chem. Soc.* **86,** 5355 (1964).
13. Myerly, R. C., and Weinberg, K. G., *J. Organ. Chem.* **31,** 2008 (1966).
14. Wedler, G., Colb, K. G., Heinrich, W., and McElhiney, G., *Appl. Sur. Sci.* **2,** 85 (1978).